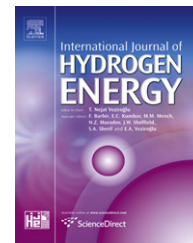




ELSEVIER

Available online at www.sciencedirect.com

SciVerse ScienceDirect

journal homepage: www.elsevier.com/locate/he

Highly hydrogen permeable Nb–Ti–Co hypereutectic alloys containing much primary bcc-(Nb, Ti) phase

Weimin Luo^{a,b,*}, Kazuhiro Ishikawa^b, Kiyoshi Aoki^b

^a Guangzhou Institute of Energy Conversion Chinese Academy of Sciences, Nengyuan Rd. 2, Tianhe, Guangzhou 510640, China

^b Graduate School of Kitami Institute of Technology, 165 Koen-cho, Kitami, Hokkaido 090-8507, Japan

ARTICLE INFO

Article history:

Received 27 March 2012

Received in revised form

27 May 2012

Accepted 1 June 2012

Available online 5 July 2012

Keywords:

Hydrogen embrittlement

Hydrogen absorption

Hydrogen permeation

Hydride

Phase transformation

ABSTRACT

In order to develop alloys combing high hydrogen permeability with large resistance to the hydrogen embrittlement, microstructures and hydrogen permeability (ϕ) have been investigated for the as-cast alloys on the straight line connecting the eutectic {TiCo + (Nb, Ti)} phase and the Nb-rich primary (Nb, Ti) phase in the Nb–Ti–Co system. The alloys on the above-mentioned line consist of the TiCo compound and the (Nb, Ti) solid solution. The value of ϕ increases with increasing temperature and volume fraction of the primary (Nb, Ti) phase. The most Nb-rich Nb₆₀Ti₂₁Co₁₉ alloy shows the highest ϕ value of 3.99×10^{-8} (mol H₂m⁻¹ s⁻¹ Pa^{-0.5}) at 673 K, which is 2.6 times higher than that of pure Pd. The present work demonstrates that highly hydrogen permeable alloys are obtainable in the Nb rich Nb–Ti–Co ones on the straight line connecting the eutectic {TiCo + (Nb, Ti)} phase and the Nb-rich primary (Nb, Ti) phase.

Copyright © 2012, Hydrogen Energy Publications, LLC. Published by Elsevier Ltd. All rights reserved.

1. Introduction

Currently hydrogen is mainly prepared by methane steam reforming (MSR) [1,2], to get pure hydrogen, separation and purification is indispensable. Pd–Ag alloys are commercially used for the separation and the purification of hydrogen gas [3]. However, Pd is very expensive and rare natural resources. Then, it is strongly desired to develop low cost and high performance hydrogen permeation alloys other than Pd alloys [4]. Generally, hydrogen permeation alloys must have high hydrogen permeability (ϕ) and high mechanical strength to endure the pressure difference between upstream and downstream side [5–10]. The product of the diffusion coefficient (D) and the solubility coefficient (K) express hydrogen permeability ϕ . High ϕ requires the

high D and/or high K . The Group 5A metals such as V, Nb and Ta have much higher hydrogen permeability than Pd–Ag alloys, but these alloys suffer from the severe hydrogen embrittlement. Generally, the high value of K gives rise to the severe hydrogen embrittlement. That is, hydrogen embrittlement is generally incompatible with high ϕ in pure metals or single-phase alloys. Recently, the present authors have found out that resistance to the hydrogen embrittlement is compatible with high ϕ in the Nb–Ti–Ni alloys consisting of the B2–TiNi and bcc-(Nb, Ti) solid solution [11–13]. The eutectic phase {TiNi + (Nb, Ti)} has large resistance to the hydrogen embrittlement and much lower hydrogen permeability than Nb, while the primary bcc-(Nb, Ti) phase contributes mainly to hydrogen permeation in this alloy. As for the Nb–Ti–Ni alloys, the hydrogen permeability should

* Corresponding author. Guangzhou Institute of Energy Conversion Chinese Academy of Sciences, Nengyuan Rd. 2, Tianhe, Guangzhou 510640, China Tel.: +86 20 3724 6316; fax: +86 20 8705 7729.

E-mail address: luowm@ms.giec.ac.cn (W. Luo).

0360-3199/\$ – see front matter Copyright © 2012, Hydrogen Energy Publications, LLC. Published by Elsevier Ltd. All rights reserved.
<http://dx.doi.org/10.1016/j.ijhydene.2012.06.005>

depend on the amount of the primary bcc-(Nb, Ti) phase, which have been verified with the Nb–Ti–Ni Hypereutectic Alloys [14]. That is, the Nb–Ti–Ni alloys have opened a new field for the hydrogen permeation membrane. It is reasonable to infer that the Nb–Ti–Co alloys containing much amount of primary bcc-(Nb, Ti) solid solution show high hydrogen permeability and large resistance to the hydrogen embrittlement. According to the previous works, the further improvement of ϕ could be may achieve by the increment of the volume fraction of the primary (Nb, Ti) phase. Ternary alloys on the straight line connecting the eutectic point and the primary phase in the phase diagram consist of the eutectic and primary phases. The constituting phases of the Nb₄₀Ti₃₀Co₃₀ alloy, i.e. the primary (Nb, Ti) phase and the eutectic {(Nb, Ti) + TiCo} phase, are Nb₈₇Ti₈Co₅ and Nb₃₀Ti₃₅Co₃₅, respectively. Hydrogen permeability ϕ of the Nb-rich Nb–Ti–Co alloys on the line connecting the eutectic point and the primary phase in the Nb–Ti–Co phase diagram are investigated in order to find out high performance hydrogen permeable alloys.

2. Experimental

The Nb-rich Nb–Ti–Co alloys on the straight line connecting the eutectic point (Nb₃₀Ti₃₅Co₃₅) and the primary phase (Nb₈₇Ti₁₃Co₄) in the Nb–Ti–Co phase diagram were prepared by arc melting using Nb (99.9 mass% purity), Ti (99.5 mass% purity) and Co (99.9 mass%) in a purified argon atmosphere. In the present work, alloy compositions are expressed by mol%. Disk samples of 12 mm in diameter and 0.8 mm in thickness were cut from the alloy ingots with a spark erosion wire-cutting machine. Both sides of disks were polished with buff and α -alumina of 0.5 μ m particle, and coated with Pd in the thickness of 190 nm by an RF-sputtering machine. Microstructural observations and structural examinations were carried out using a scanning electron microscope (SEM) and a powder X-ray diffractometer (XRD). Chemical compositions were analyzed by an energy dispersive X-ray spectrometer (EDS) attached to SEM. The volume fracture of primary (Nb, Ti)

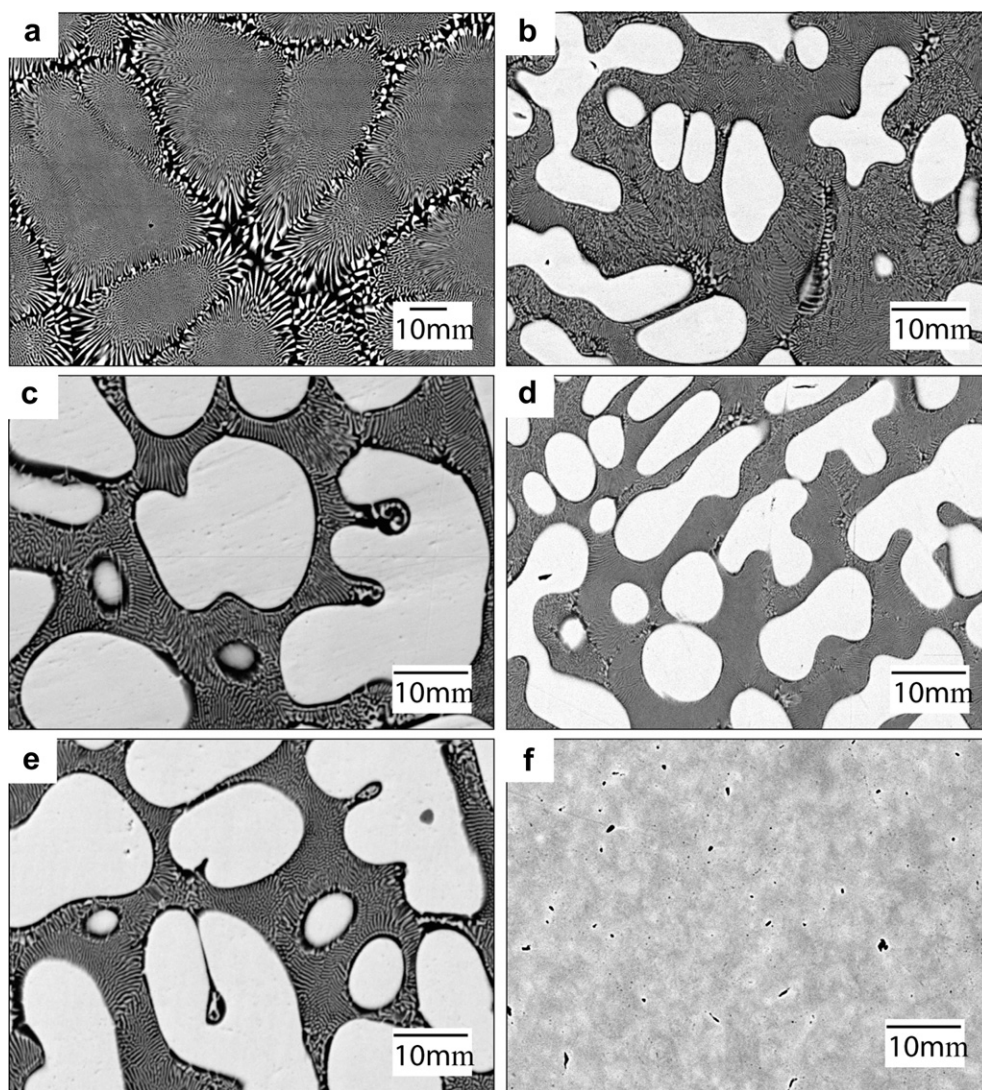


Fig. 1 – The SEM photographs of the Nb–Ti–Co alloys on the straight line connecting the eutectic point and the primary phase. (a) The Nb₃₀Ti₃₅Co₃₅, (b) the Nb₄₈Ti_{26.5}Co_{25.5}, (c) the Nb₅₆Ti₂₃Co₂₁, (d) the Nb₆₀Ti₂₁Co₁₉, (e) the Nb₆₄Ti₁₉Co₁₇ alloy and (f) the Nb₈₆Ti₁₁Co₄ alloys.

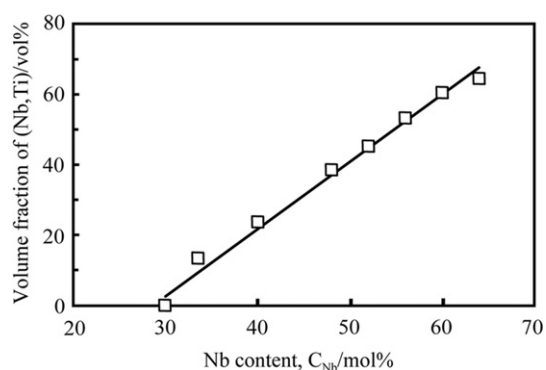


Fig. 2 – The volume fraction of the primary (Nb,Ti) phase increases proportionately with the Nb contents for the Nb–Ti–Co alloys on the straight line connecting the eutectic point and the primary phase.

phase was achieved by analyzing the SEM photograph with the public domain NIH image program. The XRD pattern of the Pd-coated disk sample was firstly measured at 673 K in a vacuum. The Pd-coating was done to avoid oxidation and to promote the hydrogen dissociation and the recombination. Hydrogen permeability ϕ was measured by using the apparatus, which has been described in the previous paper [11]. The hydrogen flux J was measured for above upstream pressure, respectively. The measurements were repeated when the temperature was stepped down from 673 K to 523 K at 50 K intervals.

3. Results

3.1. Microstructures and the crystal structure of Nb–Ti–Co alloys on the line connecting the eutectic and the primary phase compositions

Fig. 1(a)–(f) show scanning electron microscopic (SEM) photograph of the Nb–Ti–Co alloys on the straight line

connecting the compositions of the eutectic and the primary phases, i.e., the $\text{Nb}_{30}\text{Ti}_{35}\text{Co}_{35}$, the $\text{Nb}_{48}\text{Ti}_{26.5}\text{Co}_{25.5}$, the $\text{Nb}_{56}\text{Ti}_{23}\text{Co}_{21}$, the $\text{Nb}_{64}\text{Ti}_{19}\text{Co}_{17}$ and the $\text{Nb}_{83}\text{Ti}_{13}\text{Co}_4$ alloys in the as-cast state, respectively. An SEM photograph of the $\text{Nb}_{30}\text{Ti}_{35}\text{Co}_{35}$ alloy shows the fine lamellar microstructure characteristic of the eutectic phase, while that of the $\text{Nb}_{83}\text{Ti}_{13}\text{Co}_4$ one does the single-phase microstructure of the primary phase. The white phases in Fig. 1(b)–(e) are the primary (Nb, Ti) one, which are surrounded by the dark phase of the lamellar eutectic phase.

Fig. 2 shows the relation between the volume fraction of the primary (Nb, Ti) phase and the Nb content. The volume fraction of the primary phase increases linearly with increasing Nb contents of these alloys. The constituting phases of the alloys on the line connecting the compositions of the eutectic and the primary phases and their chemical compositions are tabulated in Table 1. These alloys consist of the eutectic phase and the eutectic phase + primary phase. The Nb contents in the primary phase and in the eutectic phase increase slightly with increasing Nb content in the alloys. On the contrary, Ti contents in them decrease slightly with Nb content in the alloys. The Co contents in both phases are nearly constant.

Fig. 3 shows the XRD patterns of the above-mentioned alloys. All of these alloys consist of the bcc-(Nb, Ti) and the B2–TiCo phase. From Figs. 1 and 3, we can see that these alloys consist of the eutectic {bcc-(Nb, Ti) + B2–TiCo} phase, phase, and a combination of the primary bcc-(Nb, Ti) phase with the eutectic {bcc-(Nb, Ti) + B2–TiCo} phase and the primary bcc-(Nb, Ti). The lattice parameters of the former and the latter phase are 0.330 and 0.301 nm independent of the alloy compositions, respectively.

3.2. Hydrogen permeability Φ of the Nb–Ti–Co alloys on the line connecting the eutectic and the primary phases

Fig. 4 shows the plot of $(J \times L)$ versus $(P_u^{0.5} - P_d^{0.5})$ for the above-mentioned alloys between 523 K and 673 K. The linear relation coefficient R^2 is obtained by a linear regression analysis. The R^2 values are over 0.992 in the temperature range of 523–673 K.

Table 1 – The constituting phases and their chemical compositions in the Nb–Ti–Co alloys on the straight line connecting the eutectic point and the primary phase.

Alloy	Alloy composition (nominal) (mol%)			Constituting phase	Chemical composition of the constituting phases (mol%)		
	Nb	Ti	Co		Nb	Ti	Co
$\text{Nb}_{30}\text{Ti}_{35}\text{Co}_{35}$	30	35	35	(Nb, Ti) + TiCo	30	35	35
$\text{Nb}_{40}\text{Ti}_{30}\text{Co}_{30}$	40	30	30	(Nb, Ti)	83	13	4
$\text{Nb}_{48}\text{Ti}_{26.5}\text{Co}_{25.5}$	48	26.5	25.5	(Nb, Ti) + TiCo	31	34	35
				(Nb, Ti)	83	13	4
$\text{Nb}_{52}\text{Ti}_{25}\text{Co}_{23}$	52	25	23	(Nb, Ti) + TiCo	31	33	36
				(Nb, Ti)	84	12	4
$\text{Nb}_{56}\text{Ti}_{23}\text{Co}_{21}$	56	23	21	(Nb, Ti) + TiCo	32	32	36
				(Nb, Ti)	84	12	4
$\text{Nb}_{60}\text{Ti}_{21}\text{Co}_{19}$	60	21	19	(Nb, Ti) + TiCo	33	32	35
				(Nb, Ti)	86	11	3
$\text{Nb}_{64}\text{Ti}_{19}\text{Co}_{17}$	64	19	17	(Nb, Ti) + TiCo	33	31	36
				(Nb, Ti)	86	11	3
$\text{Nb}_{83}\text{Ti}_{13}\text{Co}_4$	83	13	4	(Nb, Ti) + TiCo	33	31	36
				(Nb, Ti)	86	11	3

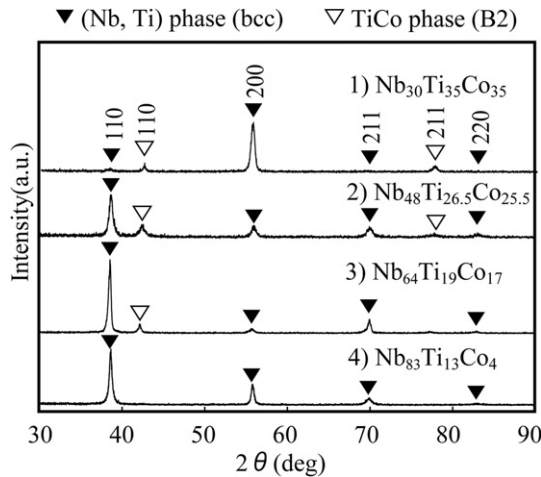


Fig. 3 – The XRD patterns of the $\text{Nb}_{30}\text{Ti}_{35}\text{Co}_{35}$, the $\text{Nb}_{48}\text{Ti}_{26.5}\text{Co}_{25.5}$, the $\text{Nb}_{64}\text{Ti}_{19}\text{Co}_{17}$, and the $\text{Nb}_{83}\text{Ti}_{13}\text{Co}_4$ alloys, respectively on the straight line connecting the eutectic point and the primary phase.

Therefore, it is reasonable to say that hydrogen permeation is controlled by the diffusion of hydrogen atoms in the alloys. The ϕ value of the alloy is determined from the slope of the line.

Fig. 5 shows hydrogen permeability ϕ of the above-mentioned alloys in the form of the Arrhenius plot. Those of Pd measured using the same apparatus and procedures as the present work are also plotted for reference in this figure. The ϕ value increases with increasing temperature and the Nb content. The values of ϕ for the Nb–Ti–Co alloys having the Nb contents between 30 and 60 mol% are higher than that of the pure Pd between 423 K and 673 K. $\text{Nb}_{60}\text{Ti}_{21}\text{Co}_{19}$ alloy shows the highest ϕ of 3.99×10^{-8} ($\text{mol H}_2\text{m}^{-1} \text{s}^{-1} \text{Pa}^{-0.5}$) at 673 K, which is 2.5 times higher than that of the pure Pd. On the other hand, the hydrogen permeation measurement is impossible due to the hydrogen embrittlement in the $\text{Nb}_{64}\text{Ti}_{19}\text{Co}_{17}$ and the $\text{Nb}_{83}\text{Ti}_{13}\text{Co}_4$ alloys.

Fig. 6 shows the values of ϕ for the above-mentioned alloys at 673 K plotted against the volume fraction of the primary phase (Nb, Ti). The ϕ value increases parabolically with increasing the volume fraction of the primary phase (Nb, Ti). The most Nb-rich hydrogen permeable $\text{Nb}_{60}\text{Ti}_{21}\text{Co}_{19}$ alloy

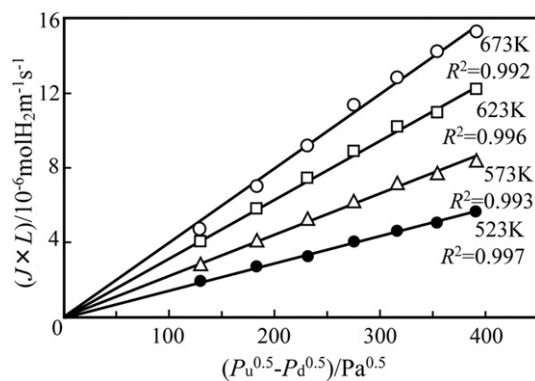


Fig. 4 – The plots of $(J \times L)$ versus $(P_u^{0.5} - P_d^{0.5})$ for the $\text{Nb}_{60}\text{Ti}_{21}\text{Co}_{19}$ alloy between 523 K and 673 K.

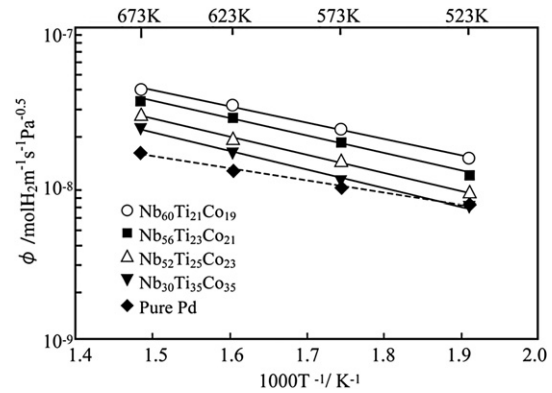


Fig. 5 – Hydrogen permeability ϕ for the as-cast Nb–Ti–Co alloys on the straight line connecting the eutectic point and the primary phase in the form of the Arrhenius plot.

consists of the 38 vol% eutectic phase and the 62 vol% primary phase.

4. Discussion

The alloy compositions investigated in the present work along with the previous one [11] are plotted in Fig. 7. The open circles and triangles denote the alloys for which the hydrogen permeation experiments are possible. On the other hand, the solid squares and circles denote the brittle alloys in the as-cast state and the broken ones by hydrogenation, respectively. According to the previous work, ϕ of the Nb–Ti–Co alloys increase with the volume fraction of the primary (Nb, Ti) phase. Consequently, in order to develop high hydrogen permeability alloys, the Nb-rich Nb–Ti–Co ones consisting of a combination of the primary phase with the eutectic phase are investigated, because the $\text{Nb}_{30}\text{Ti}_{35}\text{Co}_{35}$ eutectic alloy shows higher ϕ than the $\text{Nb}_{20.5}\text{Ti}_{38.5}\text{Ni}_{41}$ eutectic alloy. Microstructures and the ϕ values of the alloys on the straight line connecting the eutectic point and the primary phase on the Nb–Ti–Co phase diagram have been investigated. The above mentioned alloys are all consisted of bcc-(Nb,Ti) phase and eutectic {bcc-(Nb,Ti) + B2–TiCo} phase, the former

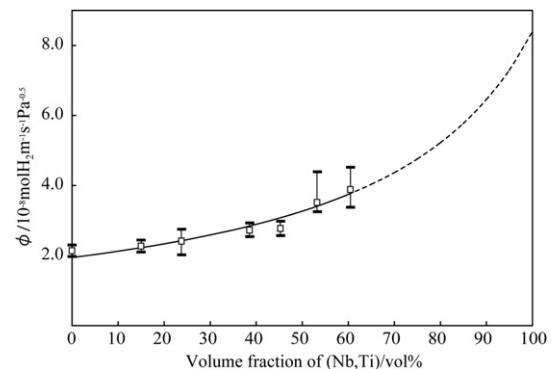


Fig. 6 – The values of ϕ for the as-cast alloys on the straight line connecting the eutectic point and the primary phase at 673 K plotted against the volume fraction of the primary phase (Nb, Ti).

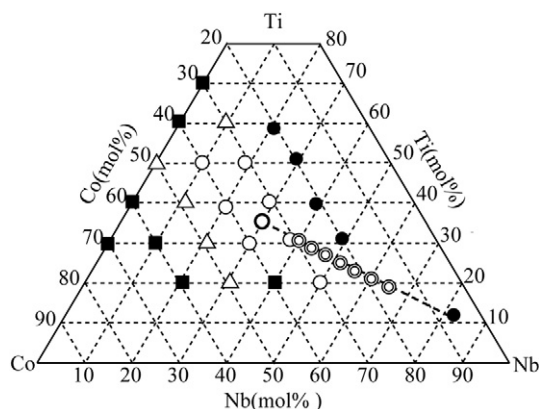


Fig. 7 – The alloy compositions investigated in the present work along with the previous one [12]. The open circles (○) and triangles (△) denote the alloys for which the hydrogen permeation experiments are possible. On the other hand, the solid squares (■) and circles (●) denote the brittle alloys in the as-cast state and the broken ones by hydrogenation, respectively.

surrounded by the latter. The Co contents of both phases show nearly constant value for all these alloys, however the Nb contents of both phases increase with the Nb contents of the alloys, and Ti contents of both phases decrease correspondently. The ϕ value increases parabolically with increasing the volume fraction of the primary phase (Nb, Ti). In fact however the $\text{Nb}_{64}\text{Ti}_{19}\text{Co}_{17}$ alloy is immeasurable in a hydrogen permeation experiment. The eutectic phase {TiCo + (Nb, Ti)} contributes to large resistance to the hydrogen embrittlement, while the primary bcc-(Nb, Ti) phase contributes mainly to hydrogen permeation in this alloy. The $\text{Nb}_{64}\text{Ti}_{19}\text{Co}_{17}$ alloy has too less amount of the eutectic phase {TiCo + (Nb, Ti)} to suppress hydrogen embrittlement.

The most Nb-rich hydrogen permeable $\text{Nb}_{60}\text{Ti}_{21}\text{Co}_{19}$ alloy shows the highest ϕ of 3.99×10^{-8} ($\text{mol H}_2\text{m}^{-1} \text{s}^{-1} \text{Pa}^{-0.5}$), which is 2.5 times higher than that of the pure Pd.

5. Summary and conclusion

In order to develop alloys combing high hydrogen permeability with large resistance to the hydrogen embrittlement, microstructures, structural changes in a hydrogen atmosphere and hydrogen permeability (ϕ), i.e., the product of hydrogen diffusion coefficient (D) and hydrogen solubility coefficient (K), have been investigated for the as-cast alloys on the straight line connecting the eutectic {TiCo + (Nb, Ti)} phase and the Nb-rich primary (Nb, Ti) phase in the Nb–Ti–Co system. The volume fraction of the primary (Nb, Ti) phase increases linearly with increasing Nb content. ϕ is measurable in the alloys containing 38 vol% or more eutectic phases, which indicate that the eutectic phase suppresses the hydrogen embrittlement. The value of ϕ increases with increasing volume fraction of the primary phase when its volume fraction is about 20 vol% or more, although it is almost independent of its volume fraction when it is less than about 20 vol%. The most Nb-rich $\text{Nb}_{60}\text{Ti}_{21}\text{Co}_{19}$ alloy shows the

highest ϕ value of 3.99×10^{-8} ($\text{mol H}_2\text{m}^{-1} \text{s}^{-1} \text{Pa}^{-0.5}$) at 673 K, which is 2.6 times higher than that of pure Pd. The present work demonstrates that highly hydrogen permeable alloys are obtainable in the Nb rich Nb–Ti–Co ones on the straight line connecting the eutectic {TiCo + (Nb, Ti)} phase and the Nb-rich primary (Nb, Ti) phase.

The Nb-rich Nb–Ti–Co alloys on the line connecting the eutectic point ($\text{Nb}_{30}\text{Ti}_{35}\text{Co}_{35}$) and primary phase ($\text{Nb}_{87}\text{Ti}_8\text{Co}_5$) consist of primary bcc-(Nb, Ti) phase and eutectic {bcc-(Nb, Ti) + B2–TiCo} phase, the former surrounded by the later. The $\text{Nb}_{64}\text{Ti}_{19}\text{Co}_{17}$ alloy is immeasurable in a hydrogen permeation experiment. Hydrogen permeability ϕ of the Nb-rich Nb–Ti–Co alloys on the above-mentioned line increases with the volume fraction of the primary phase up to 62 vol%. The most Nb-rich $\text{Nb}_{60}\text{Ti}_{21}\text{Co}_{19}$ alloy, consisting of the 38 vol% eutectic phase and the 62 vol% primary phase, shows the highest ϕ of 3.99×10^{-8} ($\text{mol H}_2\text{m}^{-1} \text{s}^{-1} \text{Pa}^{-0.5}$).

REFERENCES

- [1] Tsuru T, Yamaguchi K, Yoshioka T, Asaeda M. Methane steam reforming by microporous catalytic membrane reactors. *AIChE J* 2004;50:2794–805.
- [2] Kikuchi E. Membrane reactor application to hydrogen production. *Catal Today* 2000;56:97–101.
- [3] Chen Wei-Hsin, Hsu Po-Chih, Lin Bo-Jhih. Hydrogen permeation dynamics across a palladium membrane in a varying pressure environment. *Int J Hydrogen Energy* 2010; 35:5410–8.
- [4] Mordkovich VZ, Baichtock YK, Sosna MH. The large scale production of hydrogen from gas mixtures. *Platinum Metals Rev* 1992;36:90–7.
- [5] Nishimura C, Komaki M, Amano M. Hydrogen permeation characteristics of vanadium–nickel alloys. *Mater Trans JIM* 1991;32:501–7.
- [6] Buxbaum RE, Kinney AB. Hydrogen transport through tubular membranes of palladium-coated tantalum and niobium. *Ind Eng Chem Res* 1996;35:530–7.
- [7] Nishimura C, Komaki M, Hwang S, Amano M. V–Ni alloy membranes for hydrogen purification. *J Alloys Compd* 2002; 330–332:902–6.
- [8] Zhang Y, Ozaki T, Komaki M, Nishimura C. Hydrogen permeation characteristics of vanadium–aluminium alloys. *Scr Mater* 2002;47:601–6.
- [9] Ozaki T, Zhang Y, Komaki M, Nishimura C. Hydrogen permeation characteristics of V–Ni–Al alloys. *Int J Hydrogen Energy* 2003;28:1229–35.
- [10] Zhang Y, Ozaki T, Komaki M, Nishimura C. Hydrogen permeation of Pd–Ag alloy coated V–15Ni composite membrane: effects of overlayer composition. *J Memb Sci* 2003;224:81–91.
- [11] Hashi K, Ishikawa K, Matsuda T, Aoki K. Hydrogen permeation characteristics of multi-phase Ni–Ti–Nb alloys. *J Alloys Compd* 2004;368:215–20.
- [12] Hashi K, Ishikawa K, Matsuda T, Aoki K. Microstructure and hydrogen permeability in Nb–Ti–Co multiphase alloys. *J Alloys Compd* 2006;425:284–90.
- [13] Ishikawa K, Seki Y, Kita K, Matsuda M, Nishida M, Aoki K. Hydrogen permeation in rapidly quenched amorphous and crystallized $\text{Nb}_{20}\text{Ti}_{40}\text{Ni}_{40}$ alloy ribbons. *Int J Hydrogen Energy* 2011;36:1784–92.
- [14] Luo Weimin, Ishikawa Kazuhiro, Aoki Kiyoshi. Hydrogen permeability in Nb–Ti–Ni alloys containing much primary (Nb, Ti) phase. *Mater Trans* 2005;46:2253–9.